# Feature Analysis for Parkinson's Disease Detection Based on Transcranial Sonography Image

Lei Chen[1,3], Johann Hagenah[2], and Alfred Mertins[1]

[1] Institute for Signal Processing, University of Luebeck, Germany
[2] Department of Neurology, University Hospital Schleswig-Holstein, Germany
[3] Graduate School, University of Luebeck, Germany

**Abstract.** Transcranial sonography (TCS) is a new tool for the diagnosis of Parkinson's disease (PD) according to a distinct hyperechogenic pattern in the substantia nigra (SN) region. However a procedure including rating scale of SN hyperechogenicity was required for a standard clinical setting with increased use. We applied the feature analysis method to a large TCS dataset that is relevant for clinical practice and includes the variability that is present under real conditions. In order to decrease the influence to the image properties from the different settings of ultrasound machine, we propose a local image analysis method using an invariant scale blob detection for the hyperechogenicity estimation. The local features are extracted from the detected blobs and the watershed regions in half of mesencephalon area. The performance of these features is evaluated by a feature-selection method. The cross validation results show that the local features could be used for PD detection.

**Keywords:** Parkinson's Disease, Transcranial Sonography, Blob detection, Feature analysis, local feature.

## 1 Introduction

Transcranial sonography (TCS) was used for the first time in a clinical study between a group of Parkinson's disease (PD) patients and healthy controls in 1995 [1]. For PD patients, the hyperechogenicity of the substantia nigra (SN) was significantly increased compared with controls. In 2002 the SN hyperechogenicity in PD was confirmed by another independent group [2]. By means of TCS, it is possible to determine the formation of idiopathic PD as well as monogenic forms of parkinsonism at an early state [3]. Furthermore, the SN area showed a distinct hyperechogenicity pattern on TCS for about 90% of PD patients, however, the structural abnormalities were not detected on CT and MRI scans [4]. These studies show that the SN hyperechogenicity is a valuable marker for PD diagnosis, especially for early diagnosis [5]. Compared to other clinical imaging modalities, the advantages of TCS include mobility, lack of side effects, and low cost. However, the quality of TCS images mainly dependents on the experience of the examiner and the acoustic bone window of the patient. With increased use,

N. Ayache et al. (Eds.): MICCAI 2012, Part III, LNCS 7512, pp. 272–279, 2012.

a standardized procedure including rating scale of SN echogenicity was required for a standard clinical setting [7].

One solution to reduce investigator dependence of the diagnosis is to apply feature analysis to the image of the ipsilateral mesencephalon wing, which is close to the ultrasound probe as shown in Fig. 1. Firstly, the moment of inertia and Hu1-moment were calculated based on manually segmented half of mesencephalon (HoM) for separating control subjects from Parkin mutation carriers [5]. Then a hybrid feature extraction method which includes statistical, geometrical and texture features for the early PD risk assessment was proposed [8], which showed good performance of texture features (especially Gabor features). Thirdly, a texture analysis method that applied a bank of Gabor filters and gray-level co-occurrence matrices (GLCM) was used on TCS images [9]. After feature selection by sequential forward floating selection (SFFS), GLCM texture features were combined with Gabor features as a feature subset. The cross validation showed good results with the selected feature subset.

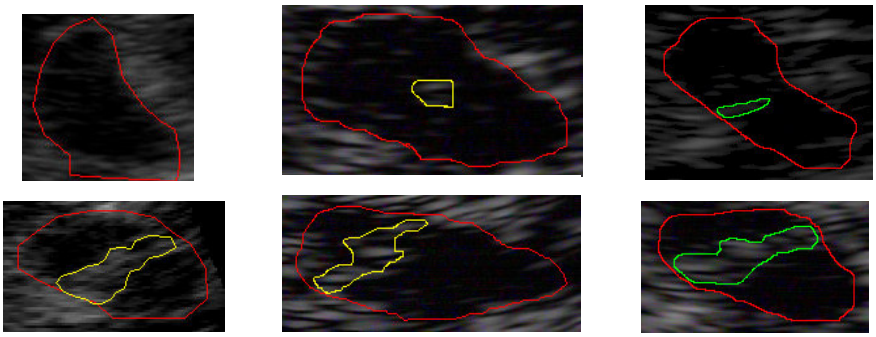

(a) Images from dataset1 (b) Images from dataset2 (c) Images from dataset3

**Fig. 1.** Manually segmented TCS images from Philips SONOS 5500. The first row is from healthy control subjects, and the second row from PD patients. The red marker indicates the upper HoM. Yellow/green markers show the SN area as a bright spot.

The last two previous works [8,9] analyzed data from only one ultrasound machine, and the selected features turned out to be sensitive to user settings and the ultrasound machine itself. In this paper, we collected three datasets that were acquired by different examiners with Philips SONOS 5500 in different periods. These datasets include the TCS images from PD and the healthy controls (HC). Actually, the properties of the TCS images, such as the gray values, the brightness, and the contrast, could be possibly affected by the different settings of the ultrasound machine used by different examiners. The mean and variance of the region of interest (HoM) in each TCS image were calculated and shown in Fig. 2. The variation between each dataset can be seen from TCS images in Fig. 1 and the statistical features of the images in Fig. 2. Our goal is to develop local features that are invariant to the illumination and contrast changes from

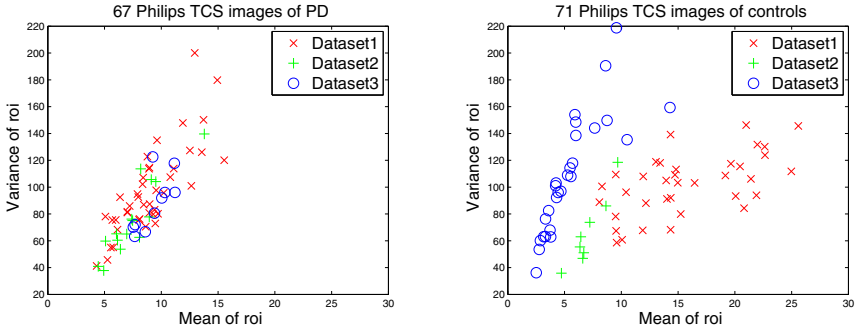


(a) 38 subjects of Parkinson's Disease (b) 39 subjects of healthy control

**Fig. 2.** The illustration about mean and variance of ROI (HoM) of 138 TCS images from Philips SONOS 5500

the different settings, even invariant to different ultrasound machines. The proposed local feature analysis method applies invariant blob detection to localize the hyperechogenicity area in HoM area and extracts local features based on watershed regions for the hyperechogenicity estimation.

## 2 Keypoint Localization

The hyperechogenicity of SN area consists of several bright spots in TCS image. The blob detection algorithm is stable under the monotonic changes in gray scale. The goal of this section is to localize the hyperechogenicity in HoM by the invariant scale blob detector. Based on space-scale theory, a multi-scale blob detector was proposed by Lindeberg [10], which could automatically select the appropriate scale for an observation. The scale space can be built using differential operators, such as Laplacian of Gaussian (LoG) and difference of Gaussians (DoG) filters. A brief framework for the invariant scale blob detector based on LoG is given by

$$\bigtriangledown^2_{\text{norm}}\, g = \sigma^2 \cdot \bigtriangledown^2 g(x, y; \sigma). \tag{1}$$

where $\sigma$ is the standard deviation of the Gaussian $g(x, y; \sigma)$, and the scale-space representation $L(x, y; \sigma)$ of the image $f(x, y)$ is defined as

$$L(x, y; \sigma) = \bigtriangledown^2_{\text{norm}} g * f(x, y), \tag{2}$$

$$(\hat{x}, \hat{y}; \hat{\sigma}) = \arg[\text{extremum}_{(x,y;\sigma)} L(x, y; \sigma)], \tag{3}$$

where $(\hat{x}, \hat{y})$ corresponds to the center vector and $\hat{\sigma}$ to the scale vector of the detected blobs on each scale level. We suppose that one blob center $(\hat{x}_1, \hat{y}_1)$ is stable through the scale space, and a unique maximum over scales is given by

$$\partial_\sigma(L(\hat{x}_1, \hat{y}_1; \sigma)) = 0. \tag{4}$$

The evolution of blobs along scales was studied based on the idealized model patterns [10]. In practice, the amount of detected blobs on each scale level is different, and the centers of the same blobs might not be found at the same position on corresponding levels. One common solution is that a blob is detected if a local 3D extreme is present and its absolute value is higher than a threshold [11]. However, same blobs at different scales are not related and can be detected many times along the scale space. Our strategy is to link the trajectory of the same blobs along scale space and select the scale and center at the unique maxima that best represent each blob. For the presentation of this method, a phantom image was created as shown in Fig. 3(c). The linked pipelines for each detected blob from the phantom image are shown in Fig. 3(a). The corresponding local maxima of each pipe through scales are shown in Fig. 3(b). The final scale selection by (4) is shown in Fig. 3(c).

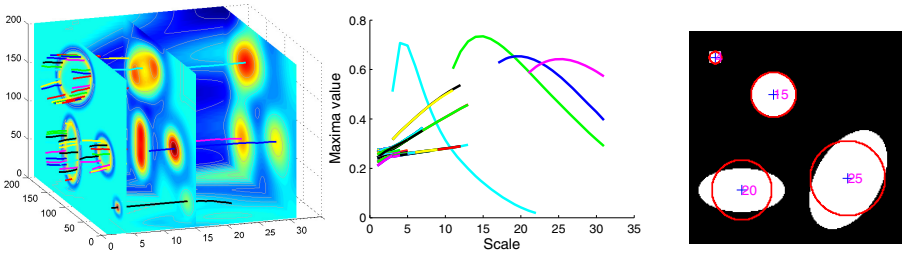


(a)Pipes through scale space (b)Extrema of the pipes (c)Scale selection result

**Fig. 3.** Blob scale selection from their trajectories along scale-space representation with LoG. (a) Three filtered images at scale $\sigma = 4$, 15, and 30. (b) Four global maxima at scales 4, 15, 20, and 25 were found from the connected trajectories. (c) Four corresponding blobs were detected and displayed on the phantom image.

In addition, the DoG is a close approximation to the scale normalized LoG, $\bigtriangledown^2_{norm} g$, given by

$$g(x, y; k\sigma) - g(x, y; \sigma) \approx (k - 1) \bigtriangledown^2_{\text{norm}} g, \tag{5}$$

where the factor $(k - 1)$ is constant over all scales and has almost no impact on the stability of extrema localization [12]. In this paper, DoG was applied for the construction of scale space. Actually, the analysis of scale-space maxima presents severe complications in TCS image, but the possible hyperechogenicity areas are localized by the proposed extrema selection method.

## 3 Local Feature Extraction

The mesencephalon is a butterfly-shape-like structure from the transverse view. The TCS image is obtained from the temporal acoustic bone window in a standardized axial mesencephalic imaging plane [5]. Only the HoM which is close to

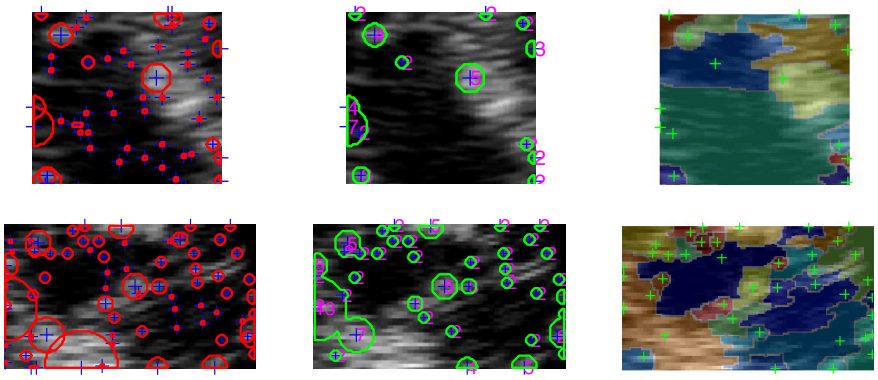

(a) Maxima in 26 neighbors (b) Maxima in pilpeline (c) Watershed regions

**Fig. 4.** (a) Detected maxima using DoG in 26 neighbors or (b) through pipe in scale space from control images (top row) and PD (bottom row) of Philips SONOS 5500. (c) Watershed segmentation results based on the detected blobs.

the probe is analyzed because of a decreased signal-to-noise ratio with increasing insonation depth. As a result, two TCS images from both sides are acquired per individual. It is better for this study not to include uncertainties that are attributed to the segmentation algorithm. Therefore HoM images were manually segmented by physicians and then analyzed for the estimation of the hyperechogenicity. The hyperechogenicity area is indicated with the blob detection as shown in Fig. 4. In the next step, a local image descriptor is needed to label the detected blob. The watershed algorithm [13] works on the gradient of an image, which is invariant to the brightness changes of the image. The watershed regions were thus segmented with the input of the detected blobs to estimate the hyperechogenicity in HoM.

Firstly, the blobs were detected with DoG operators in the HoM using the proposed extrema-selection method. The detection results of TCS images from Philips SONOS 5500 are shown in Fig. 4. The same blobs were prevented from being detected many times and the appropriate scales for each blob are indicated around the blob center as shown in Figs. 4(a) and (b). Secondly, based on the input of the detected blobs, the watershed regions were segmented and labeled by different color as shown in Fig. 4(c). Then, a selection procedure for the blob and watershed region was implemented with an ellipse mask filtering the false positives as shown in Fig. 5(a). From the prior knowledge of the anatomic location of SN, this mask is created from the ellipse which is fitted onto the ROI as mentioned in [5]. The values of the ellipse mask are calculated from their distance $d$ to the minor ellipse axis. For $d < f$ (with $f$ the distance between the focus point and the minor axis) the mask value is one. For $d \geq f$ the mask value is zero. Only the blobs that have big scale (For example, $\sigma \geq 3$) were taken into account as shown in Fig. 5(b). The watershed regions that are entirely within the ROI were considered as interesting areas. As a result, the selected blobs (indicated by green plus signs) and watershed regions are shown in Fig. 5(c).

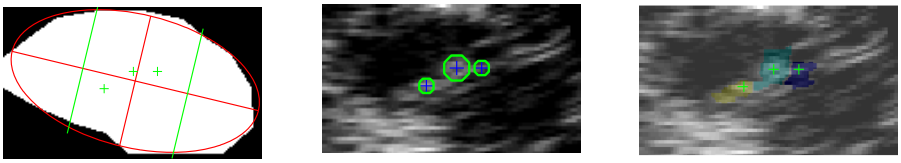

(a) Ellipse mask (b) Selected blobs (c) Selected regions

**Fig. 5.** (a) An ellipse is fitted with the ROI. Two green lines are parallel to the minor ellipse axis and across the two ellipse focuses, respectively. (b) The selected blobs (green sign) and (c) the selected watershed regions which are inside of the ellipse mask.

For the estimation of the hyperechogenicity, nine local features $F1...F9$ were extracted based on the selected blobs and watershed regions in HoM. Entropy is used to measure the randomness of a local region. The parameters shape and scale of a Weibull approximation [14] of the gradient distribution were determined by maximum likelihood estimation [13] and used as local image features. The calculation of entropy and the estimation of Weibull distribution parameters were obtained from the gradient images after Gaussian smoothing. Considering the image scaling, the features F1 and F2 were normalized by the corresponding HoM area. The local features are shown as follows:

F1,F3: Area and entropy of all selected watershed regions
F2,F4: Area and entropy of all selected blobs
F5,F6: Weibull parameters (a,b) of all selected watershed regions and blobs
F7: The scale of the biggest detected blob
F8,F9: Entropy of the biggest blob and HoM

## 4 Experimental Results

The experiments were based on three data sets which were obtained with Philips SONOS 5500 by different examiners. Dataset 1 includes 42 TCS images from 23 PD patients and 36 TCS images from 21 healthy controls. Dataset 2 includes 15 PD TCS images from ten PD patients and eight control images from four controls. The last dataset consisted of ten PD TCS images from five PD patients and 27 TCS from 14 controls. Totally, this large dataset includes 67 PD images from 38 PD patients and 71 control images from 39 healthy subjects.

The outline of the framework is as follows: First, the dataset is classified using the selected feature subsets F(17, 25, 26, 27, 29) from [8] and F(17, 77) from [9]. Secondly, based on the manually segmented HoM images which were marked by the physicians, the suspicious hyperechogenicity areas were localized by the invariant scale blob detection method. Then, the watershed-segmentation algorithm was applied to the gradient image after Gaussian smoothing. At last, local features were extracted based on the selected blobs and the watershed regions. These local features were evaluated by the feature-selection method SFFS. The criterion function of SFFS was the accuracy of the SVM classifier.

The training of SVMs was carried out with sequential minimal optimization (SMO) and a linear kernel. The SVM classification results were cross validated with the leave-one-out method.

The feature analysis results are shown in Table 1. Based on this dataset, the features found in [8] and [9] achieved 76.81% and 48.55% correct rate, respectively. Five local features $F(3,7,8,1,9)$ were selected with SFFS based on this dataset. Using the selected local featrues, the classification accuracy reached 72.46%, which was better than the Gabor feature and GLCM feature from [9]. To test how the feature sets perform when standard operations such as brightness and contrast normalization are carried out, for each image the intensity values in the ROI were normalized to the range $[0, 255]$. The results in the right column of Table 1 show that the local features are invariant to illumination changes from the image normalization and outperform the other features under such conditions.

In another experiment, an SVM classifier was used to evaluate the performance of the three selected feature subsets when the training is carried out on other datasets than the test. We used Datasets 1 and 3 for Training and Dataset 2 for test. The classification results are listed in Table 2. They show that the classifier with the selected local features works better than the others when training and test conditions are different.

**Table 1.** Feature analysis and SVMs cross-validation results on the large dataset

| Dataset 1,2,3 | Accuracy | Confusion matrix | Accuracy(normalized data) |
|---|---|---|---|
| $F(17, 25, 26, 27, 29)$ from [8] | 76.81% | $\begin{pmatrix} 63 & 4 \\ 28 & 43 \end{pmatrix}$ | 71.01% |
| $F(17, 77)$ from [9] | 48.55% | $\begin{pmatrix} 40 & 27 \\ 44 & 27 \end{pmatrix}$ | 58.70% |
| Local feature $F(3, 7, 8, 1, 9)$ | 72.46% | $\begin{pmatrix} 52 & 15 \\ 23 & 48 \end{pmatrix}$ | 72.46% |

**Table 2.** Classification results of the three selected feature subsets

| Training data(Dataset 1,3), test data (Dataset2) | Accuracy | Confusion matrix |
|---|---|---|
| $F(17, 25, 26, 27, 29)$ from [8] | 65.22% | $\begin{pmatrix} 15 & 0 \\ 8 & 0 \end{pmatrix}$ |
| $F(17, 77)$ from [9] | 60.87% | $\begin{pmatrix} 14 & 1 \\ 8 & 0 \end{pmatrix}$ |
| Local feature $F(3, 7, 8, 1, 9)$ | 78.26% | $\begin{pmatrix} 14 & 1 \\ 4 & 4 \end{pmatrix}$ |

## 5 Conclusions

We have analyzed the selected features from two previous works and nine new local features based on a large dataset of TCS images. In particular, the local features are invariant to the monotonic changes in gray scale. Almost all possible locations of hyperechogenicity in HoM area could be indicated by the proposed

invariant scale blob detection. Moreover, the watershed segmentation was applied to segment the ROI for PD detection. Of course, the current results depend on the manual segmentation of HoM area by physician. An automatic segmentation algorithm could be implemented for localization of the HoM area. Even though the appearance of mesencephalon can vary considerably across subjects, the prior knowledge of anatomic shape and location of SN can be utilized for the improvement of the selection strategy. The keypoint detection would be improved with shape estimation, and more robust and precise local image descriptors of hyperechogenicity may be developed for PD detection.

## References


1. Becker, G., Seufert, J., Bogdahn, U., Reichmann, H., Reiners, K.: Degeneration of substantia nigra in chronic Parkinson's diseasvisualized by transcranial color-coded real-time sonograph. Neurology 45, 182–184 (1995)
2. Walter, U., Wittstock, M., Benecke, R., Dressler, D.: Substantia nigra echogenicity is normal in non-extrapyramidal cerebral disorders but increased in Parkinson's disease. J. Neural Transm. 109, 191–196 (2002)
3. Behnke, S., Berg, D., Becker, G.: Does ultrasound disclose a vulnerability factor for Parkinson's disease? J. Neural 250(suppl.1), I24–I27 (2003)
4. Hagenah, J.M., Hedrich, K., Becker, B., Pramstaller, P.P., Seidel, G., Klein, C.: Distinguishing early-onset PD from dopa-responsive dystonia with transcranial sonography. Neurology 66, 1951–1952 (2006)
5. Kier, C., Seidel, G., Bregemann, N., Hagenah, J., Klein, C., Aach, T., Mertins, A.: Transcranial Sonography as Early Indicator for Genetic Parkinson's Disease. In: Vander Sloten, J., Verdonck, P., Nyssen, M., Haueisen, J. (eds.) ECIFMBE 2008. IFMBE Proceedings, pp. 456–459. Springer, Heidelberg (2009)
6. Kier, C., Cyrus, C., Seidel, G., Hofmann, U., Aach, T.: Segmenting the substantia nigra in ultrasound images for early diagnosis of Parkinson's disease. International Journal of Computer Assisted Radiology and Surgery 2, S83 (2007)
7. Berg, D., Steinberger, J.D., Warren Olanow, C., Naidich, T.P., Yousry, T.A.: Milestones in Magnetic Resonance Imaging and Transcranial Sonography of Movement Disorders. Movement Disorders 26 (2011)
8. Chen, L., Seidel, G., Mertins, A.: Multiple Feature Extraction for Early Parkinson Risk Assessment Based on Transcranial Sonography Image. In: Proceedings of 2010 IEEE 17th International Conference on Image Processing (2010)
9. Chen, L., Hagenah, J.M., Mertins, A.: Texture Analysis Using Gabor filter Based on Transcranial Sonography Image. In: Bildverarbeitung Für die Medizin 2011, pp. 249–253 (2011)
10. Lindeberg, T.: Feature Detection with Automatic Scale Selection. International Journal of Computer Vision 30(2) (1998)
11. Ferraz, L., Binefa, X.: A Scale Invariant Interest Point Detector for Discriminative Blob Detection. In: Araujo, H., Mendonça, A.M., Pinho, A.J., Torres, M.I. (eds.) IbPRIA 2009. LNCS, vol. 5524, pp. 233–240. Springer, Heidelberg (2009)
12. Lowe, D.G.: Distinctive image features from scale-invariant keypoints. International Journal of Computer Vision 60, 91–110 (2004)
13. Meyer, F.: Topographic distance and watershed lines. Signal Processing 38, 113–125 (1994)
14. Devroye, L.: Non-Uniform random variate generation. Springer, New York (1986)